JVI Journals.ASM.org

Protective Role of Interferon Regulatory Factor 3-Mediated Signaling against Prion Infection

Daisuke Ishibashi,[a] Ryuichiro Atarashi,[a,c] Takayuki Fuse,[a] Takehiro Nakagaki,[a] Naohiro Yamaguchi,[a] Katsuya Satoh,[a] Kenya Honda,[b] and Noriyuki Nishida[a,d]

Department of Molecular Microbiology and Immunology, Nagasaki University Graduate School of Biomedical Sciences, Nagasaki, Japan[a]; Department of Immunology, Graduate School of Medicine and Faculty of Medicine, University of Tokyo, Tokyo, Japan[b]; Nagasaki University Research Centre for Genomic Instability and Carcinogenesis, Nagasaki, Japan[c]; and Global Centers of Excellence Program, Nagasaki University, Nagasaki, Japan[d]

Abnormal prion protein (PrP^{Sc}) generated from the cellular isoform of PrP (PrP^{C}) is assumed to be the main or sole component of the pathogen, called prion, of transmissible spongiform encephalopathies (TSE). Because PrP is a host-encoded protein, acquired immune responses are not induced in TSE. Meanwhile, activation of the innate immune system has been suggested to partially block the progression of TSE; however, the mechanism is not well understood. To further elucidate the role of the innate immune system in prion infection, we investigated the function of interferon regulatory factor 3 (IRF3), a key transcription factor of the MyD88-independent type I interferon (IFN) production pathway. We found that IRF3-deficient mice exhibited significantly earlier onset with three murine TSE strains, namely, 22L, FK-1, and murine bovine spongiform encephalopathy (mBSE), following intraperitoneal transmission, than with wild-type controls. Moreover, overexpression of IRF3 attenuated prion infection in the cell culture system, while PrP^{Sc} was increased in prion-infected cells treated with small interfering RNAs (siRNAs) against IRF3, suggesting that IRF3 negatively regulates PrP^{Sc} formation. Our findings provide new insight into the role of the host innate immune system in the pathogenesis of prion diseases.

Transmissible spongiform encephalopathies (TSE) are fatal zoonoses and include Creutzfeldt-Jakob disease (CJD) in humans, and scrapie and bovine spongiform encephalopathy (BSE) in animals. All exhibit the three major histopathological features of spongiform change, neuronal loss, and gliosis in the central nervous system (CNS) (30). The infectious agent, prion, is considered not to possess its own genome and to be composed mainly of the proteinase K (PK)-resistant and β-sheet-rich abnormal isoform of prion protein, designated PrP^{Sc}, which is generated by conformational conversion of the normal form of PrP (PrP^{C}) (43). In contrast to responses to conventional pathogens, such as bacteria and viruses, acquired immunity against prion infection is not elicited, probably because PrP is a host-encoded protein, resulting in immunotolerance to PrP^{Sc} (1).

Prior to activation of acquired immune responses, the invasion of pathogens, including bacteria and viruses, is first recognized by the innate immune system, with the switching on of the cellular defense system leading to the production of cytokines and interferons (IFNs). The innate immune responses are initiated through both Toll-like receptors (TLRs) (2) and intracellular sensor molecules such as retinoic acid inducible gene-I (RIG-I) and melanoma differentiation-associated gene-5 (MDA5), each of which recognizes specific components of foreign pathogens, namely, pathogen-associated molecular patterns (PAMPs) (20). In addition, the innate immunity is the main system contributing to inflammation caused by microbial infection or tissue damage (3, 8). Since gliosis, a major characteristic of TSE, is thought to be a kind of inflammatory response, it is reasonable to assume that innate immunity may play a role in the pathogenesis of TSE. Indeed, it was reported that pretreatment with complete Freund's adjuvant (CFA) (39) or unmethylated CpG DNA (35), both of which activate innate immunity through TLRs, delays the onset of TSE in mice inoculated with mouse-adapted scrapie prion, suggesting that activation of innate immunity is protective against prion infection. In contrast, deletion of the MyD88 gene, which is an essential intracellular signal transducer in all TLRs except for TLR3, has been shown not to significantly affect incubation time in the same mouse scrapie model (29). Thus, MyD88-dependent signaling pathways are unlikely to be implicated in prion infection in the absence of forced activation of innate immune responses by conventional PAMPs (2, 20). On the other hand, mice that possess a nonfunctioning mutation of TLR4, which activates not only the MyD88-dependent but also the MyD88-independent (also called TRIF-dependent) pathway, develop scrapie earlier than control mice (36). Accordingly, it is suggested that blockade of the TLR4 signaling pathway accelerates the progression of TSE. Nonetheless, the effects of the innate immune system on prion infection remain controversial and have not been fully clarified.

We focus on interferon regulatory factor 3 (IRF3), which is a key transcription factor of the MyD88-independent pathway that has an essential role in the type I IFN response to microbial infection and whose deficiency in mice leads to susceptibility to many viruses (19). In this study, we investigated the role of IRF3 in prion infection using IRF3-deficient mice and prion-susceptible cell lines.

MATERIALS AND METHODS

Reagents and antibodies. The anti-PrP polyclonal mouse antiserum (SS) has been described previously (5). M20 is an affinity-purified goat polyclonal antibody recognizing the C terminus of mouse PrP (Santa Cruz

Received 16 September 2011 Accepted 16 February 2012
Published ahead of print 29 February 2012
Address correspondence to Daisuke Ishibashi, dishi@nagasaki-u.ac.jp.

doi:10.1128/JVI.06326-11

Biotechnology, Inc., CA). Anti-mouse IRF3 (Santa Cruz Biotechnology) and anti-mouse phospho-IRF3 (Ser396) (Cell Signaling Technology, Japan) were rabbit polyclonal antibodies, and anti-mouse β-actin (Sigma-Aldrich, St. Louis, MO) was a mouse monoclonal antibody. Horseradish peroxidase (HRP)-conjugated anti-goat immunoglobulin G antibody (Santa Cruz Biotechnology) and anti-mouse and anti-rabbit IgG antibodies (Amersham Pharmacia Biotech AB, Uppsala, Sweden) were used for Western blotting.

Cell cultures. The mouse neuroblastoma cell line N2a was purchased from the American Type Culture Collection (ATCC CCL131), and N2a58 cells overexpressing mouse PrP prepared from N2a were transfected with a plasmid carrying wild-type mouse *prnp* cDNA (PrP-a genotype, codons 108L and 189T) (27). Prion-infected cells, 22L-N2a58, were produced as previously described (27). After limiting dilution, several PrP^{Sc}-positive clones were isolated. The cell clones producing the highest level of PrP^{Sc} were used for subsequent studies. The 22L-N2a58 cells stably expressed PrP^{Sc} for over 50 passages. The cells were cultured in Dulbecco's modified Eagle's medium (DMEM; Sigma) containing 10% heat-inactivated fetal bovine serum and penicillin-streptomycin (Invitrogen, Carlsbad, CA) and split every 3 days at a 1:10 ratio. All cultured cells were maintained at 37°C in 5% CO_2 in the biohazard prevention area of Nagasaki University.

Plasmid and siRNA. The mammalian pUNO expression vector contains a strong and ubiquitous composite promoter designated EF1α/human T-cell leukemia virus (HTLV). In this experiment, we inserted mouse IRF3 cDNA into multiple cloning sites of the pUNO vector (InvivoGen, San Diego, CA). The hemagglutinin (HA)-tagged mouse IRF3 cDNA was inserted into the pcDNA3.1 vector (Invitrogen). The plasmids were introduced by Lipofectamine LTX (Invitrogen) in the prion-infected cells and incubated for 48 h. The small interfering RNAs (siRNAs) were purchased from Qiagen, Hilden, Germany. Two specific siRNA-targeted sequences (product numbers SI00210770 and SI00210784) were used for IRF3 (according to GenBank accession number NM016849): 5′-ACA GGT GGT GAT GGT TGG CAA-3′ and 5′-GAC CCT TAT GAC CCT CAT AAA-3′. For the negative control, an siRNA (product 1022076) targeting 5′-AAT TCT CCG AAC GTG TCA CGT-3′ was used. The siRNAs were introduced into cells using Fugene 6 (Roche Diagnostics, Mannheim, Germany) and incubated for 48 h.

Western blotting. Samples were lysed with Triton-deoxycholate (DOC) lysis buffer (50 mM Tris-HCl [pH 7.5] containing 150 mM NaCl, 0.5% Triton X-100, 0.5% sodium deoxycholate, 2 mM EDTA, and protease inhibitors [Nakarai Tesque, Inc., Japan]) for 30 min at 4°C. After 1 min of centrifugation at 5,000 × *g*, the supernatant was collected, and its total protein concentration was measured using a bicinchoninic acid (BCA) protein assay kit (Pierce, Rockford, IL). To detect PrP^{Sc}, the protein concentration was adjusted to 10 mg/ml, and samples were digested with 20 μg/ml of proteinase K (PK; Sigma) at 37°C for 30 min, boiled for 5 min with sodium dodecyl sulfate (SDS) loading buffer (50 mM Tris-HCl, pH 6.8, containing 5% glycerol, 1.6% SDS, and 100 mM dithiothreitol), and subjected to SDS-polyacrylamide gel electrophoresis. The proteins were transferred onto an Immobilon-P membrane (Millipore, MA) in transfer buffer containing 15% methanol at 300 mA for 1 h; the membrane was blocked with 5% nonfat dry milk in TBST (10 mM Tris-HCl [pH 7.8], 100 mM NaCl, 0.1% Tween 20) for 1 h at room temperature and reacted with diluted primary antibodies. Immunoreactive bands were visualized by HRP-conjugated secondary antibodies, using an enhanced chemiluminescence system (Amersham). The detailed methods have previously been described (4). To quantify the signals, we measured the intensity of each band using NIH ImageJ software.

Establishment of stably IRF3-overexpressing cells and *in vitro* 22L scrapie infection experiments. To establish cell lines stably expressing IRF3, pcDNA3.1 plasmid containing an HA-tagged IRF3 gene was transfected using Fugene 6 (Roche) into PrP^{C}-overexpressing N2a cells (N2a75 cells) and cultured for 48 h. After the cells were treated with 350 μg/ml hygromycin (HygroGold; InvivoGen) in culture medium for 4 days, the drug-resistant colonies were isolated. We used the HygroGold-selected N2a75 cells transfected with an empty vector as a negative control. Then, the cells were infected with the 22L scrapie strain (final concentration, 0.02 or 0.2% brain homogenate [BH]) in a six-well culture plate for 48 h and subsequently passaged into a 75-cm^2 flask. Once confluent, the subcultures were diluted 10-fold (27). After treatment with 40 μg/ml PK, immunoblotting was done to detect PrP^{Sc}.

***In vivo* scrapie infection experiments.** Four-week-old wild-type (+/+) and IRF3 knockout (−/−) male mice of the same C57BL/6-derived genetic background were intraperitoneally (i.p.) inoculated with 100 μl of a 10^{-3} dilution of brain homogenate from mice terminally infected with 22L, Fukuoka-1 (FK-1), or a mouse-adapted BSE (mBSE) strain (28). The $IRF3^{-/-}$ mice were obtained from T. Taniguchi's group (Tokyo University) (33). As a negative (mock-infected) control, age- and strain-matched mice were inoculated i.p. with normal mouse BH. The spleens and brains of the mice were removed at 1, 2, 5, 8, and 25 weeks postinfection (wpi) and at the terminal stage of disease. Animals were cared for in accordance with the Guidelines for Animal Experimentation of Nagasaki University.

Histopathology and immunohistochemical staining. The spleen and brain tissues were fixed in 4% paraformaldehyde, and 5-μm paraffin sections were prepared on poly-L-lysine (PLL)-coated slides with a microtome. To measure vacuolation in brain, the tissue sections were stained with hematoxylin and eosin (HE). In PrP^{Sc} staining, after deparaffinization and rehydration, the sections were pretreated by hydrated autoclaving at 121°C for 15 min in 1 or 1.2 mM hydrochloric acid (17), followed by immersion in 90% formic acid for 5 min (25) to enhance PrP visualization, according to the protocol described by Brown et al. (9). Endogenous peroxidase activity was inhibited with 0.3% hydrogen peroxidase in methanol for 30 min. Nonspecific binding sites of the primary antibody SAF32 (Spi-Bio, Montigny le Bretonneux, France) was blocked by preincubation in normal rabbit serum at 1:20 (Dako, Glostrup, Denmark) for 30 min and then optimally titrated and diluted to 1:5,000 and 1:500 (26, 32). The negative-control sections were incubated with normal mouse IgG1 and IgG2b serum (Dako) and then exposed to the primary antibodies overnight at room temperature. For determining the follicular dendritic cell (FDC) population in the spleen, we used anti-FDC antibody CNA.42 (Dako) (31) and normal mouse IgM serum (Dako) as a negative control for primary antibodies and a Histofine mouse stain kit (Nichirei Biosciences, Inc., Japan) for the secondary antibody. In glial staining, primary antibodies of anti-glial fibrillary acidic protein (GFAP) (Dako) for the detection of activated astrocyte and anti-Iba-1 (Wako, Japan) for activated microglia were used. The secondary antibodies were Envision-mouse or rabbit HRP (Dako) used at 1:200 for 1 h. Finally, the samples were stained with 0.025% 3,3′-diaminobenzidine (DAB; Dojindo Lab, Japan) to visualize the reaction product and counterstained with hematoxylin. The patterns of vacuolation, PrP^{Sc} deposits, and gliosis were examined in five areas, namely, the cortex, hippocampus, thalamus, cerebellum, and Pons. In semiquantitative evaluation of spongiosis and gliosis, lesion severity of vacuolation as spongiform degeneration was scored on a scale of 0 to 5 (nondetectable, few, mild, moderate, severe, and status spongiosus, respectively). PrP^{Sc} deposit was scored on a scale of 0 to 4 (nondetectable, few, mild, moderate, and severe, respectively). Microgliosis and astrogliosis were scored on a scale of 0 to 3 (nondetectable, mild, moderate, and severe, respectively), and the values for each brain region were averaged.

Statistical analysis. The Student *t* test and Mann-Whitney U-test were used for comparison between two groups, and one-way analysis of variance (ANOVA) followed by a Tukey-Kramer test was used for multiple comparisons. A log rank test was used to analyze mortality of prion-infected mice. The correlation between parameters was determined by simple regression analysis and Pearson's correlation coefficient test. Statistical analysis of all data was performed using Statcel, version 2, on Excel and GraphPad Prism software.

TABLE 1 Survival periods of prion-infected wild-type and IRF3 knockout mice

Strain	Survival period (days) by mouse group[a]	
	Wild type $(n)^b$	IRF3$^{-/-}$ $(n)^b$
22L	281 ± 15 (9)	257 ± 8 (5)***
BSE	380 ± 33 (7)	335 ± 37 (7)*
FK-1	321 ± 24 (4)	251 ± 31 (5)**

[a] Animals were intraperitoneally administrated a 10^{-3} dilution of brain homogenate from prion-infected terminal mice. Values are average ± standard deviation. *, $P < 0.05$; **, $P < 0.01$; ***, $P < 0.001$ (Student t test).
[b] n, number of mice.

RESULTS

Prion infection is accelerated in IRF3-deficient mice. To clarify the significance of IRF3-dependent signaling pathways in prion infection *in vivo*, we peripherally inoculated the 22L strain into IRF3 gene knockout mice (IRF3$^{-/-}$) (33) and control wild-type (C57BL/6) mice. When the mice were challenged with a 10^{-3} dilution of 22L inoculum by the intraperitoneal (i.p.) route, the IRF3$^{-/-}$ mice showed significantly abbreviated survival periods (257 ± 8 days; $P < 0.001$) compared with those of the control mice (281 ± 15 days) (Table 1 and Fig. 1A). To further investigate the protective effect of IRF3 on prion infection, the mice were challenged with a 10^{-3} dilution of a mouse-adapted BSE (mBSE) or Fukuoka 1 (FK-1) strain by the i.p. route. IRF3$^{-/-}$ mice showed shorter survival periods of mBSE (335 ± 37 versus 380 ± 33 days; $P < 0.05$) and FK-1 (251 ± 31 versus 321 ± 24 days, $P < 0.01$) than the control mice (Table 1). The shortening of survival periods in the IRF3$^{-/-}$ mice is unlikely to be due to developmental defects in the brains or lymphoreticular organs because IRF3$^{-/-}$ mice were shown to have normal lymphocyte populations in the thymus and spleen (33). Moreover, immunostaining with antifollicular dendritic cell (FDC) antibody (CNA.42) (31) was performed to compare the FDC population in the spleen between IRF3$^{-/-}$ and wild-type mice. Staining reactions were similar in the two groups (see Fig. 4B).

We examined the presence of PrP^{Sc} in the brain tissues of terminal-stage mice infected with the 22L prion strain by Western blotting. The levels of PrP^{Sc} in IRF3$^{-/-}$ mice at 32 weeks p.i. (wpi) were equivalent to those of wild-type mice at 40 wpi (Fig. 1B). Moreover, no significant differences were observed between wild-type mice and IRF3$^{-/-}$ mice in the accumulation of PrP^{Sc} in the lesion profiles of PrP immunostaining (Fig. 1C). Because spongiform changes and gliosis are common characteristics of prion diseases, brain sections including the cerebral cortex, hippocampus, thalamus, cerebellum, and pons (Po) from 22L-inoculated mice were examined histologically and subjected to immunohistochemical analysis using anti-Iba-1 antibodies for microgliosis (Fig. 2A) or anti-GFAP for astrogliosis (Fig. 2B). The severity and distribution of vacuolation and glial activation in the IRF3$^{-/-}$ mice at 32 wpi were indistinguishable from those in the wild-type mice at 40 wpi (Fig. 2 and 3), while IRF3$^{-/-}$ mice displayed sig-

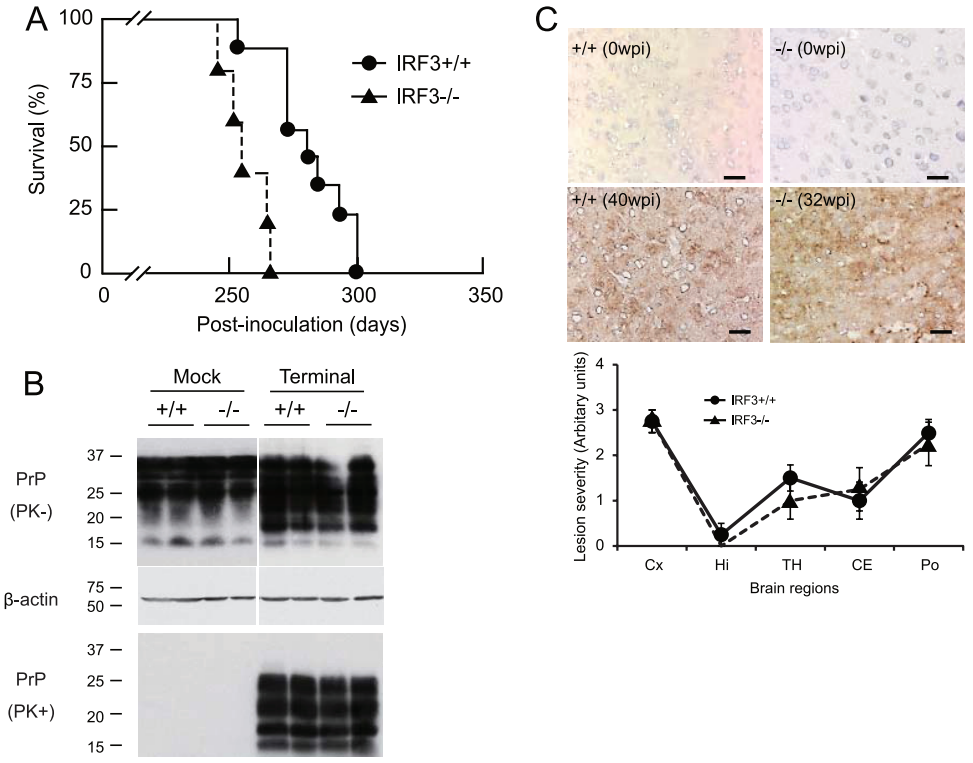

FIG 1 Acceleration of prion pathogenesis in IRF3$^{-/-}$ mice. (A) Survival curves in wild-type (+/+) ($n = 9$) and IRF3 knockout (−/−) ($n = 5$) mice after i.p. inoculation of a 10^{-3} dilution of 22L-BH are plotted. The difference between the two groups is statistically significant ($P < 0.05$, log rank test). (B) Accumulation of PrP^{Sc} in the brain tissues from wild-type or IRF3$^{-/-}$ mice was analyzed by Western blotting. Molecular mass markers are indicated (in kDa) on the left side of each panel. (C) PrP^{Sc} deposits were similarly stained in the cortex area of wild-type (+/+) and IRF3 knockout (−/−) mice at the terminal stages (upper panels). There were no significant differences between wild-type and IRF3$^{-/-}$ mice in the staining levels of PrP^{Sc} in the five brain regions: cortex (Cx), hippocampus (Hi), thalamus (TH), cerebellum (CE) and pons (Po) (lower graph). Scale bar, 25 μm. All data are representative of at least three mice.

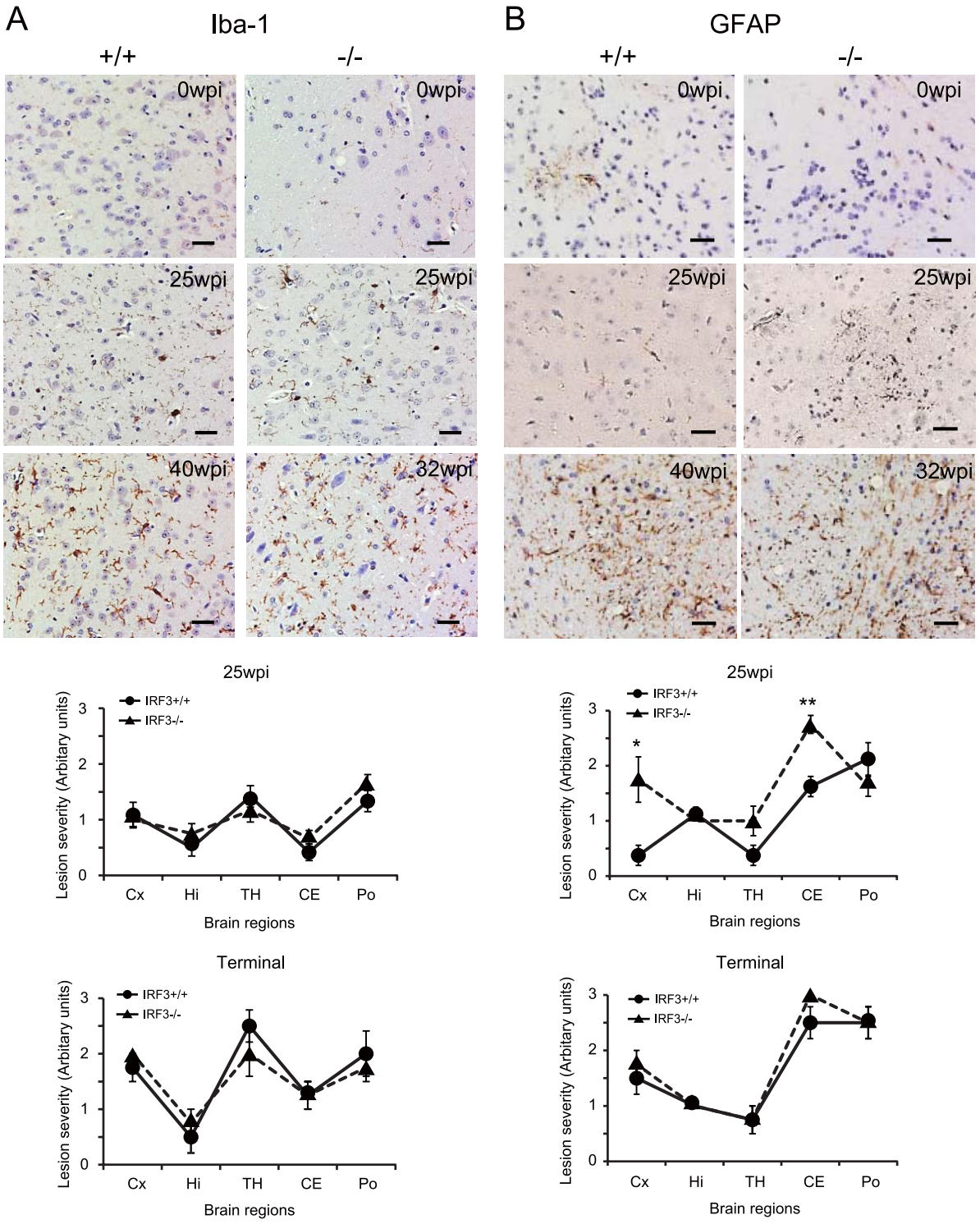

FIG 2 Histopathological examination of gliosis in the brains of prion 22L-infected mice. (A) Immunohistochemical staining for Iba-I with hematoxylin counterstaining was performed. The sections of cortex (Cx) from wild-type (+/+) and IRF3 knockout (−/−) mice at 0 and 25 wpi and at terminal stages are shown (upper panels). Lesion profiles of microgliosis in the same five brain regions as shown in Fig. 1B were compared between the prion-inoculated wild-type and IRF3$^{-/-}$ mice at the terminal stages (lower graph). No significant differences were observed between the two groups at 25 wpi or at the terminal stage. (B) Immunostaining for GFAP with hematoxylin counterstaining (upper panels) and lesion profiles of astrogliosis (lower graph). Significant differences were observed between the two groups in cortex and cerebellum (CE) regions at 25 wpi but not at the terminal stage. Statistical significance was determined using a two-tailed Student's *t* test. **, $P < 0.01$; *P, < 0.05 (compared with wild-type mice). Error bars indicate standard error of the mean. Scale bar, 25 μm. All results are representative of at least three mice.

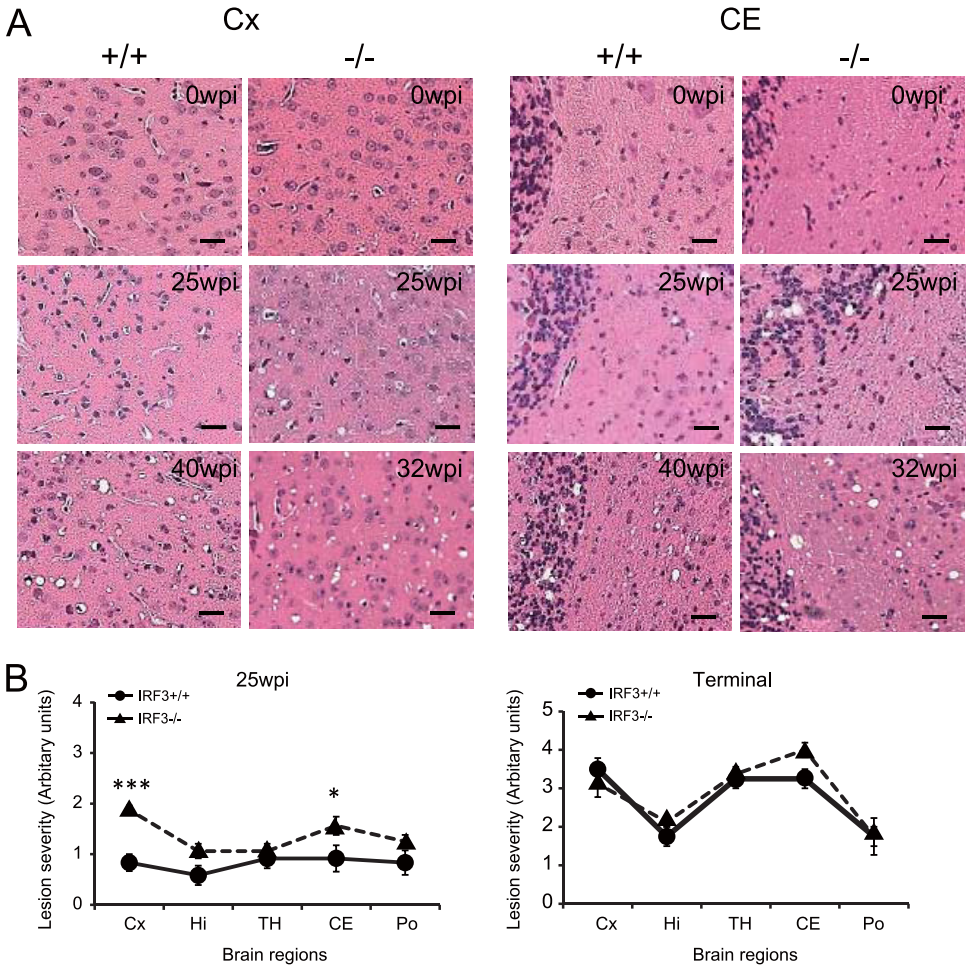

FIG 3 Comparison of spongiform change between wild-type and IRF3$^{-/-}$ mice after 22L prion infection. (A) Sections of the cortex (Cx) and cerebellum (CE), stained with hematoxylin and eosin, from wild-type (+/+) and IRF3 knockout (−/−) mice at 0 and 25 wpi and at terminal stages after i.p. inoculation of a 10^{-3} dilution of 22L-BH are shown. Scale bar, 25 μm. (B) Vacuolation scores in the same five brain regions as shown in Fig. 1B were compared between the prion-inoculated wild-type and IRF3$^{-/-}$ mice at 25 wpi or the terminal stages. Statistical significance was determined using a two-tailed Student's *t* test. ***, $P < 0.001$; *, $P < 0.05$ (compared with wild-type mice). Error bars indicate standard error of the mean. These results are representative of at least three mice.

nificantly increased vacuolation (Fig. 3) and astrogliosis (Fig. 2B) in the cerebral cortex and cerebellum at 25 wpi. Collectively, these results suggest that the progression of TSE following i.p. transmission is accelerated in IRF3$^{-/-}$ mice although genetic elimination of IRF3 does not affect the final neuropathological outcome. Furthermore, as shown in Table 2 and Fig. 4A, the deposition of PrP^{Sc} in the white pulp region of the spleens from the IRF3$^{-/-}$ mice was detectable in 1/5 mice at 2 wpi, 4/5 at 5 wpi, and 5/5 at 8 wpi, whereas none of the wild-type mice was positive at the same time points. These observations indicate that the rate of accumulation of PrP^{Sc} in the spleen was enhanced in the IRF3$^{-/-}$ mice.

TABLE 2 PrP^{Sc}-positive rate in the spleens in mice with i.p. inoculation of 22L at the indicated time points

Period postinoculation (no. of wks or stage)	No. of PrP^{Sc}-positive mice/total no. of mice[a]	
	Wild type	IRF3$^{-/-}$
1	0/5	0/1
2	0/5	1/5
5	0/5	4/5
8	0/5	5/5
Terminal	1/1	1/1

[a] The presence of PrP^{Sc} accumulation in the spleen of prion-infected mice was determined by immunohistochemical staining.

The IRF3-dependent pathway is protective against prion infection in cell culture. We tested whether overexpression of IRF3 could affect the production of PrP^{Sc} in the cell culture models. The level of PrP^{C} was not affected by the transient expression of the genes in uninfected N2a58 cells (data not shown). PrP^{Sc} was significantly decreased by overexpression of IRF3 in the 22L-N2a58 cells (Fig. 5A). We confirmed that the activated form of IRF3 (phosphorylated at Ser396 of IRF3) increases in a dose-dependent manner after transfection of the IRF3 gene in both 22L-N2a58 cells (Fig. 5A) and uninfected N2a58 cells (data not shown), indicating that the upregulation of IRF3 phosphorylation seen in the Fig. 5A is most likely due to an increase in the level of IRF3 protein after transfection.

To investigate the effect of downregulation of IRF3 in the 22L-N2a58 cells, we performed knockdown experiments using small

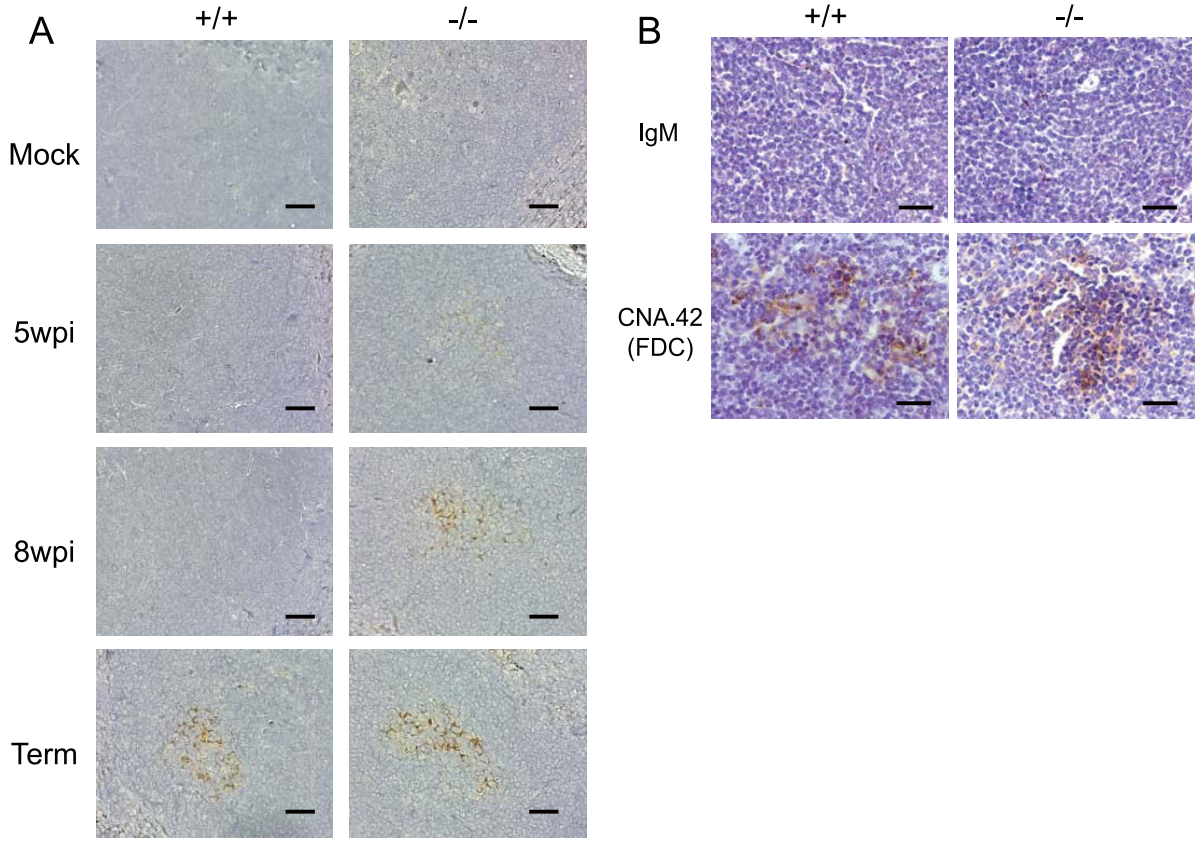

FIG 4 Early detection of PrP^{Sc} deposits in the spleen of prion-inoculated $IRF3^{-/-}$ mice. (A) Accumulation of PrP^{Sc} in the spleens was analyzed by immunohistochemistry (hydrophobic autoclaving method) at 5 and 8 wpi and at terminal stages after i.p. inoculation of a 10^{-3} dilution of 22L-BH. Scale bar, 25 μm. (B) The sections of spleen from wild-type (+/+) and IRF3 knockout (−/−) 5-week-old mice were stained with anti-FDC antibody (CNA.42). IgM is a negative control for the primary antibody. Scale bar, 20 μm.

interfering RNAs (siRNAs). IRF3 expression was significantly decreased by two types of siRNAs against IRF3, whereas β-actin expression, as the internal standard, was not changed (Fig. 5B). Application of siRNA did not influence the expression of PrP^{C} in N2a58 cells (data not shown), whereas the level of PrP^{Sc} was increased in 22L-N2a58 cells treated with siRNA against IRF3 (Fig. 5B). These data suggest that IRF3 has an inhibitory effect on the production of PrP^{Sc} in the 22L-N2a58 cells.

To further evaluate the protective effect of IRF3, we established cell clones stably expressing HA-tagged IRF3 using another mouse PrP-overexpressing N2a cell clone (designated N2a75). Several HA-IRF3-negative and -positive clones were isolated by selection for resistance to hygromycin. HA-tagged IRF3 was expressed in clones A4, C1, and H3, which were accompanied by an increase in total IRF3 protein, while clones A1 and E1 were negative (Fig. 5C). After incubation with 22L-infected BH (22L-BH), the cell clones were subcultured for five passages and analyzed by Western blotting with anti-PrP antibodies. The values of the PrP^{Sc}/PrP^{C} ratio were inversely correlated with the values of the IRF3/beta-actin ratio (Fig. 5C), indicating that enhanced expression of IRF3 effectively blocks new prion infection.

DISCUSSION

In the present study, we found that a genetic deficiency of IRF3 accelerates the progression of TSE following i.p. transmission in mice and that the accumulation rate of PrP^{Sc} in the spleen is increased in the $IRF3^{-/-}$ mice. Furthermore, we demonstrated that IRF3 has an inhibitory effect on PrP^{Sc} accumulation and that the levels of IRF3 are inversely correlated with resistance to prion infection in cell culture.

IRF3 is known to be constitutively expressed in many tissues and cells (6, 22, 45). Indeed, we confirmed the expression of IRF3 in brains (data not shown) and N2a58 cells (Fig. 5). Furthermore, not only glial cells but also neurons express most innate immunity-related genes and produce type I IFN in response to virus infection (11). Although the role of IRF3 in prion propagation into the CNS is still unclear, we speculate that an absence of IRF3 signaling leads to increased prion replication not only in peripheral tissues but also in the CNS. It would be of great value to examine this further using neuron-specific IRF3-disrupted mice or neuron-specific IRF3-expressing mice.

It was reported in prion infection that genetic disturbance of TLR4 (36) or interleukin-10 (IL-10) (41) leads to shorter incubation periods of prion infection. Since these, respectively, are an upstream and a downstream factor of the IRF3-mediated pathway, the findings may be due in part to functional changes in IRF3-mediated signaling.

Based on these results, two hypothetical models are proposed to explain the inhibitory effect of IRF3 on the prion infection. The first is that MyD88-independent pattern recognition receptors

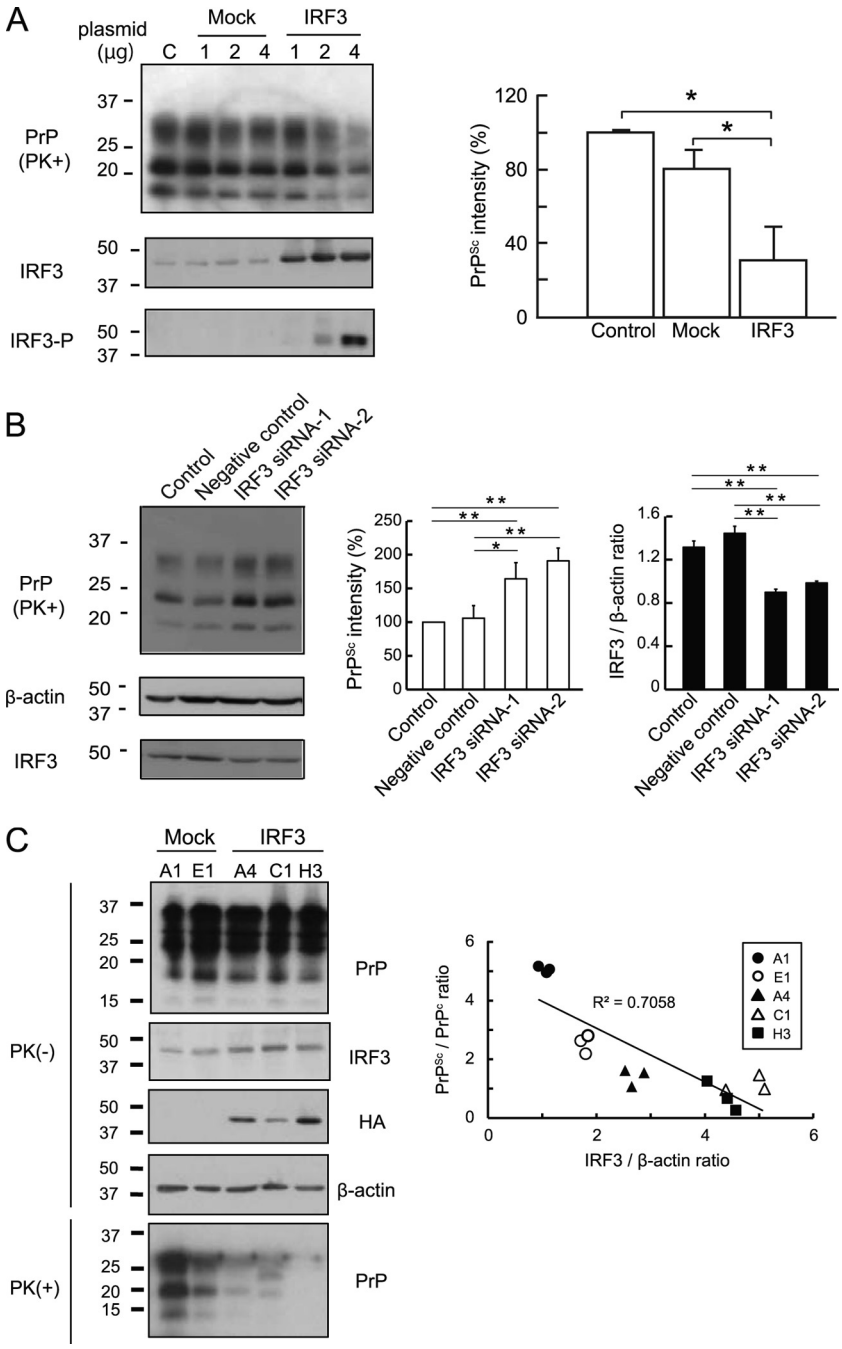

FIG 5 Inhibitory effect of IRF3 on PrP^{Sc} replication in cell culture. (A) Plasmids (pUNO) containing the IRF3 gene were transiently transfected into 22L-N2a58 cells and incubated for 48 h. The panels on the left show PK-treated PrP as PrP^{Sc}, total IRF3, and phosphorylated IRF3 (IRF3-P) in the cells. Mock, plasmids without the IRF3 gene. The numbers above the panels represent the amount (μg) of the plasmids used for transfection. C, untransfected cells for negative control. The levels of PrP^{Sc} band intensity in the cells transfected with 4 μg of the plasmids with or without the IRF3 gene are expressed as a percentage compared with the control (right graph). The results in the graph are the mean ± standard deviation of three independent experiments. Asterisks indicate statistically significant differences (*, $P < 0.05$). (B) The siRNAs of IRF3 were transfected into 22L-N2a58 cells and incubated for 48 h. The cells were subjected to Western blotting to detect PrP^{Sc}, β-actin, and IRF3. The band intensities of PrP^{Sc} or the IRF3/β-actin ratios were quantified. Asterisks indicate statistically significant differences (*, $P < 0.05$; **, $P < 0.01$). The data are representative of three independent experiments. (C) The effect of overexpression of HA-tagged IRF3 on new prion infection was analyzed using stable IRF3-overexpressing clones A4, C1, and H3. Hygromycin-resistant but IRF3-negative clones, A1 and E1, were used as the negative controls. The top four panels show protein expression of PrP^{C}, total IRF3, HA-tagged IRF3, and β-actin prior to infection in each clone. After incubation with 0.02% 22L-BH for 48 h and then five passages, PrP^{Sc} levels in the clones were determined by Western blotting. The scatter diagram is indicative of a correlative relationship between the PrP^{Sc}/PrP^{C} ratio and the IRF3 expression ratio (right graph). A statistically significant ($P < 0.001$) correlation ($r = -0.8$) was observed between the PrP^{Sc} and the IRF3/β-actin ratio. The coefficients of determination are shown as R^2 values. All results are representative of at least three independent experiments, and each experiment was performed in triplicate.

(PRRs), such as TLR3, TLR4, or RIG-I/MDA5, might recognize prion, and the resulting activation of IRF3 could induce various IRF3-responsive genes that may participate in the protective effect. The fact that the *in vivo* administration of IFNs, a representative of the IRF3-responsive genes, previously failed to show inhibitory effects on TSE (13, 16) suggests that IRF3-responsive genes other than IFNs may be important for the inhibitory effect of IRF3 on prion infection. Of note, the protective effect of IRF3 against several viruses has been suggested to be largely independent of the production of type I IFN and is probably responsible for the antiviral actions of specific IRF3-responsive genes (10, 18, 21). Peritoneal macrophages from wild-type mice moderately induced tumor necrosis factor alpha (TNF-α) or IL-6 following exposure to PrP^{Sc}-mimicking PrP peptides (PrP residues 106 to 126 or PrP residues 118 to 135), whereas TLR4 signaling-mutant mice were impaired in their ability to produce these cytokines (36), supporting in part the hypothesis that some PRRs may sense PrP^{Sc} as a sort of PAMP. On the other hand, it should be noted that the MyD88-independent pathway activates both NF-κB and IRF3. Although the induction of proinflammatory cytokines essentially depends upon NF-κB, it was unclear whether the activation of IRF3 was induced by these PrP peptides. In fact, the hallmarks of IRF3 activation, such as phosphorylation, dimerization, and cytoplasm-to-nucleus translocation of IRF3 in 22L-N2a58 cells, were not detected (data not shown). Moreover, it was previously reported that IFNs were not detected in the serum, spleens, or brains of mice infected with scrapie (44). In addition, IFN-β mRNA does not increase in the brains of CJD patients (7) or mice infected with ME7 prion strain (14). Hence, these results argue against the notion that the IRF3-mediated signaling is activated by prion infection, but it remains to be determined whether transient and weak responses are evoked at an early phase in the infection. The question as to whether IRF3-mediated signaling directly suppresses the production of PrP^{Sc} or increases its degradation also remains open.

Another explanation is that prion infection itself may have little effect on the pathway but that the basal activity of IRF3 may have some degree of inhibitory effect on prion propagation. It has been reported that IRF3 can be activated not only by viruses but also by multiple activators such as cellular stress and DNA damage (24, 34). Accordingly, it is possible that constitutive activation of IRF3, albeit at a low level, occurs in the brain even in the absence of a pathogen. This notion is further supported by the fact that constitutive, weak IFN signaling in the absence of viral infection plays a role in modifying cellular responsiveness in the immune and other biological systems (38, 40). Accumulating evidence indicates that many viruses have evolved to evade the innate immune system, including IRF3-mediated signaling (15, 23). For instance, an active mutant of IRF3 has been reported to exert a markedly suppressive effect on cellular HIV-1 infection, and administration of poly(I·C) potently inhibits HIV-1 replication in microglia through a pathway requiring IRF3. Nonetheless, HIV-1 itself does not activate IRF3 but, rather, decreases IRF3 protein in HIV-1-infected cells (12, 37). Likewise, prion infection might disturb the activation of IRF3 even though prion is considered to be largely composed of PrP^{Sc}. We are currently investigating this possibility. Furthermore, an analogy can be made between the role of IRF3 in prion infection and that of IL-10. The levels of IL-10 are not increased in the brains of scrapie-infected mice (14, 42), whereas IL-10 knockout mice are highly susceptible to the development of scrapie (41).

In conclusion, we have shown that IRF3, a key transcription factor of the MyD88-independent pathways, operates in the host defense machinery against prion infection. The findings provide new insight into understanding of the innate immunity to prion infection.

ACKNOWLEDGMENTS

We thank Tadatsugu Taniguchi for the gift of IRF3 knockout mice, Hitoki Yamanaka, Takehiro Matsubara, and Kazunori Sano for helpful discussions and critical assessment of the manuscript, and Mari Kudo, Ayumi Yamakawa, and Atsuko Matsuo for technical assistance.

This work was supported in part by the global COE Program (F12), a Grant-in-Aid for Young Scientists (B) (number 22790955) from the Ministry of Education, Culture, Sports, Science, and Technology of Japan, a grant for BSE research, and a grant-in-aid of the Research Committee of Prion Disease and Slow Virus Infection from the Ministry of Health, Labor and Welfare of Japan.

REFERENCES

1. **Aguzzi A, Polymenidou M.** 2004. Mammalian prion biology: one century of evolving concepts. Cell **116**:313–327.
2. **Akira S, Takeda K.** 2004. Toll-like receptor signalling. Nat. Rev. Immunol. **4**:499–511.
3. **Akira S, Uematsu S, Takeuchi O.** 2006. Pathogen recognition and innate immunity. Cell **124**:783–801.
4. **Arima K, et al.** 2005. Biological and biochemical characteristics of prion strains conserved in persistently infected cell cultures. J. Virol. **79**:7104–7112.
5. **Atarashi R, Sim VL, Nishida N, Caughey B, Katamine S.** 2006. Prion strain-dependent differences in conversion of mutant prion proteins in cell culture. J. Virol. **80**:7854–7862.
6. **Au WC, Moore PA, Lowther W, Juang YT, Pitha PM.** 1995. Identification of a member of the interferon regulatory factor family that binds to the interferon-stimulated response element and activates expression of interferon-induced genes. Proc. Natl. Acad. Sci. U. S. A. **92**:11657–11661.
7. **Baker CA, Lu ZY, Manuelidis L.** 2004. Early induction of interferon-responsive mRNAs in Creutzfeldt-Jakob disease. J. Neurovirol. **10**:29–40.
8. **Beutler B, et al.** 2006. Genetic analysis of host resistance: Toll-like receptor signaling and immunity at large. Annu. Rev. Immunol. **24**:353–389.
9. **Brown KL, Ritchie DL, McBride PA, Bruce ME.** 2000. Detection of PrP in extraneural tissues. Microsc. Res. Tech. **50**:40–45.
10. **Daffis S, Samuel MA, Keller BC, Gale M, Jr., Diamond MS.** 2007. Cell-specific IRF-3 responses protect against West Nile virus infection by interferon-dependent and -independent mechanisms. PLoS Pathog. **3**:e106.
11. **Delhaye S, et al.** 2006. Neurons produce type I interferon during viral encephalitis. Proc. Natl. Acad. Sci. U. S. A. **103**:7835–7840.
12. **Doehle BP, Hladik F, McNevin JP, McElrath MJ, Gale M, Jr.** 2009. Human immunodeficiency virus type 1 mediates global disruption of innate antiviral signaling and immune defenses within infected cells. J. Virol. **83**:10395–10405.
13. **Field EJ, Joyce G, Keith A.** 1969. Failure of interferon to modify scrapie in the mouse. J. Gen. Virol. **5**:149–150.
14. **Field R, Campion S, Warren C, Murray C, Cunningham C.** 2010. Systemic challenge with the TLR3 agonist poly I:C induces amplified IFNα/β and IL-1β responses in the diseased brain and exacerbates chronic neurodegeneration. Brain Behav. Immun. **24**:996–1007.
15. **Goodbourn S, Didcock L, Randall RE.** 2000. Interferons: cell signalling, immune modulation, antiviral response and virus countermeasures. J. Gen. Virol. **81**:2341–2364.
16. **Gresser I, Maury C, Chandler RL.** 1983. Failure to modify scrapie in mice by administration of interferon or anti-interferon globulin. J. Gen. Virol. **64**:1387–1389.
17. **Haritani M, Spencer YI, Wells GA.** 1994. Hydrated autoclave pretreatment enhancement of prion protein immunoreactivity in formalin-fixed bovine spongiform encephalopathy-affected brain. Acta Neuropathol. **87**:86–90.

18. **Hidmark AS, et al.** 2005. Early alpha/beta interferon production by myeloid dendritic cells in response to UV-inactivated virus requires viral entry and interferon regulatory factor 3 but not MyD88. J. Virol. **79**: 10376–10385.
19. **Hiscott J.** 2007. Triggering the innate antiviral response through IRF-3 activation. J. Biol. Chem. **282**:15325–15329.
20. **Honda K, Taniguchi T.** 2006. IRFs: master regulators of signalling by Toll-like receptors and cytosolic pattern-recognition receptors. Nat. Rev. Immunol. **6**:644–658.
21. **Honda K, et al.** 2005. IRF-7 is the master regulator of type-I interferon-dependent immune responses. Nature **434**:772–777.
22. **Karpova AY, Howley PM, Ronco LV.** 2000. Dual utilization of an acceptor/donor splice site governs the alternative splicing of the IRF-3 gene. Genes Dev. **14**:2813–2818.
23. **Katze MG, He Y, Gale M, Jr.** 2002. Viruses and interferon: a fight for supremacy. Nat. Rev. Immunol. **2**:675–687.
24. **Kim T, et al.** 1999. Activation of interferon regulatory factor 3 in response to DNA-damaging agents. J. Biol. Chem. **274**:30686–30689.
25. **Kitamoto T, Ogomori K, Tateishi J, Prusiner SB.** 1987. Formic acid pretreatment enhances immunostaining of cerebral and systemic amyloids. Lab. Invest. **57**:230–236.
26. **Liu WG, Brown DA, Fraser JR.** 2003. Immunohistochemical comparison of anti-prion protein (PrP) antibodies in the CNS of mice infected with scrapie. J. Histochem. Cytochem. **51**:1065–1071.
27. **Nishida N, et al.** 2000. Successful transmission of three mouse-adapted scrapie strains to murine neuroblastoma cell lines overexpressing wild-type mouse prion protein. J. Virol. **74**:320–325.
28. **Nishida N, Katamine S, Manuelidis L.** 2005. Reciprocal interference between specific CJD and scrapie agents in neural cell cultures. Science **310**:493–496.
29. **Prinz M, et al.** 2003. Prion pathogenesis in the absence of Toll-like receptor signalling. EMBO Rep. **4**:195–199.
30. **Prusiner, S. B.** 1998. Prions. Proc. Natl. Acad. Sci. U. S. A. **95**:13363–13383.
31. **Raymond I, Al Saati T, Tkaczuk J, Chittal S, Delsol G.** 1997. CNA.42, a new monoclonal antibody directed against a fixative-resistant antigen of follicular dendritic reticulum cells. Am. J. Pathol. **151**:1577–1585.
32. **Rosicarelli B, et al.** 2005. Migration of dendritic cells into the brain in a mouse model of prion disease. J. Neuroimmunol. **165**:114–120.
33. **Sato M, et al.** 2000. Distinct and essential roles of transcription factors IRF-3 and IRF-7 in response to viruses for IFN-alpha/beta gene induction. Immunity **13**:539–548.
34. **Servant MJ, Grandvaux N, Hiscott J.** 2002. Multiple signaling pathways leading to the activation of interferon regulatory factor 3. Biochem. Pharmacol. **64**:985–992.
35. **Sethi S, Lipford G, Wagner H, Kretzschmar H.** 2002. Postexposure prophylaxis against prion disease with a stimulator of innate immunity. Lancet **360**:229–230.
36. **Spinner DS, et al.** 2008. Accelerated prion disease pathogenesis in Toll-like receptor 4 signaling-mutant mice. J. Virol. **82**:10701–10708.
37. **Suh HS, et al.** 2009. TLR3 and TLR4 are innate antiviral immune receptors in human microglia: role of IRF3 in modulating antiviral and inflammatory response in the CNS. Virology **392**:246–259.
38. **Takaoka A, Taniguchi T.** 2003. New aspects of IFN-alpha/beta signalling in immunity, oncogenesis and bone metabolism. Cancer Sci. **94**:405–411.
39. **Tal Y, et al.** 2003. Complete Freund's adjuvant immunization prolongs survival in experimental prion disease in mice. J. Neurosci. Res. **71**:286–290.
40. **Taniguchi T, Takaoka A.** 2001. A weak signal for strong responses: interferon-alpha/beta revisited. Nat. Rev. Mol. Cell Biol. **2**:378–386.
41. **Thackray AM, McKenzie AN, Klein MA, Lauder A, Bujdoso R.** 2004. Accelerated prion disease in the absence of interleukin-10. J. Virol. **78**: 13697–13707.
42. **Tribouillard-Tanvier D, Striebel JF, Peterson KE, Chesebro B.** 2009. Analysis of protein levels of 24 cytokines in scrapie agent-infected brain and glial cell cultures from mice differing in prion protein expression levels. J. Virol. **83**:11244–11253.
43. **Weissmann C, Enari M, Klohn PC, Rossi D, Flechsig E.** 2002. Molecular biology of prions. Acta Neurobiol. Exp. (Wars.) **62**:153–166.
44. **Worthington M.** 1972. Interferon system in mice infected with the scrapie agent. Infect. Immun. **6**:643–645.
45. **Zhai J, et al.** 2008. Characterization of a novel isoform of murine interferon regulatory factor 3. Biochem. Biophys. Res. Commun. **377**:384–388.